

Furfural-Based Polyamides with Tunable Fluorescence Properties via Ugi Multicomponent Polymerization

Xue Wang,* Chang Liu, Zhihao Xing, Hongyi Suo, Rui Qu, Qingzhong Li, and Yusheng Qin*



Cite This: *Macromolecules* 2022, 55, 8857–8865



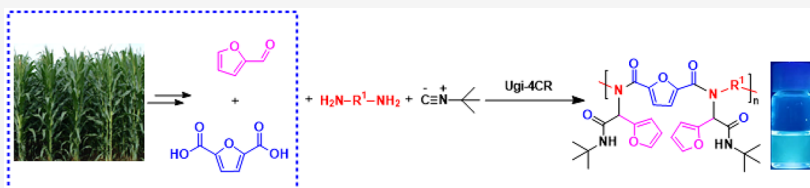
Read Online

ACCESS |

Metrics & More

Article Recommendations

Supporting Information



- Biomass-based platform molecules
- Ugi multicomponent reaction
- Modular design and atom economy
- ✓ Intramolecular hydrogen bonds
- ✓ Non-traditional intrinsic luminescence

ABSTRACT: Polyamides (PAs) are regarded as attractive fluorescent polymer materials due to their nontraditional intrinsic luminescence. In this work, a series of photoluminescence active PAs were prepared from renewable furfural derivatives via the Ugi four-component polymerization. Moreover, the fluorescence of dilute PA solutions can be accurately controlled by the intramolecular hydrogen bonding interactions using the furfural module as a switch, which was finally confirmed by DFT theory. As a probe, PAs can selectively recognize Fe^{2+} and Fe^{3+} among various metal ions by the fluorescence quenching effect. This protocol provides an efficient and moderate strategy for synthesizing biobased functional polymer materials with fluorescence properties, demonstrating high synthetic efficiency and high selectivity to Fe^{2+} and Fe^{3+} .

INTRODUCTION

With diminishing fossil resources and environmental problems caused by CO_2 emissions, researchers are actively exploiting renewable, biobased resources. In 2004, the US Department of energy first proposed 12 biomass-based platform compounds. Since then, Bozell and Petersen have supplemented them to expand them into “TOP 10 + 4” biomass-based platform compounds.¹ Among them, furfural has been identified as one of the most promising biobased platform compounds because it can be effectively produced from a hemicellulose refinery and further converted into several high-value chemicals.² Furfural derivatives, such as 1,4-butanediol and 1,5-pentanediol, can be used as feedstock in polymer synthesis. Especially, 2,5-furandicarboxylic acid (2,5-FDCA) has been successfully used as a renewable substitute for the petro-derived terephthalic acid to synthesize biobased polyesters.^{3–5} However, most of the present processes for the manufacturing of polymer monomers from furfural involve multistep reactions and thus have problems such as high cost, which limits its wide application in the field of polymerization. The development of direct polymerization methods of furfural is of great importance to achieving efficient utilization of furfural.

Multicomponent reactions (MCRs) are fascinating approaches starting from three or more reactants to prepare single polymer products in a one-pot one-step process under mild conditions.^{6–10} Among the various MCRs, Ugi-4CR with

an aldehyde (ketone), a primary amine, a carboxylic acid, and an isocyanide are widely used in polymer synthesis because of its high selectivity, atom economy, and modularity.¹¹ In 2014, Ugi-4CR was firstly introduced by Meier as a novel strategy for the synthesis of diversely substituted polyamides (PAs).¹² Also, in 2014, the Tao group applied the Ugi reaction to synthesize a series of PEGylation agents for protein conjugation.¹³ Excitingly, biobased platform compounds have great potential because of their diversity, multifunctionality, and cost-competitiveness for MCRs. Becer et al. developed a direct polymerization of renewable levulinic acid via slightly modified Ugi MCR to synthesize sustainable PAs.¹⁴ In 2019, Meier et al. documented PAs preparation based on Ugi-multicomponent polymerization of 2,5-FDCA, which was synthesized through a two-step catalytic process.¹⁵ During this period, the Tao group and Debuigne group focused on the Ugi polymerization of amino acids and dipeptides.^{16–21} Recently, Becer et al. prepared N-substituted functional PAs with $\approx 80\%$ biomass content from renewable diamine, diacid, and aldehydes via Ugi

Received: June 10, 2022

Revised: September 3, 2022

Published: September 28, 2022

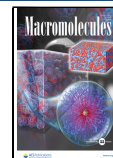
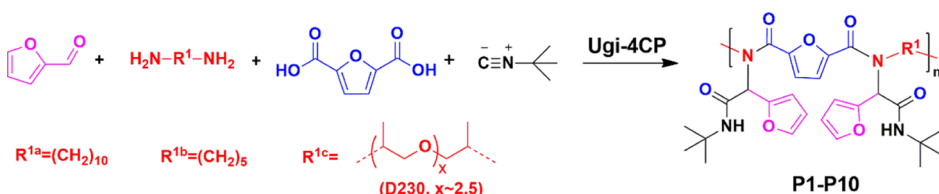


Table 1. Reaction Conditions, Molecular Weights, Polydispersities, and Yields of the Ugi-4CP

polymer	diamine monomer	concentration of diamine (mol/L) ^a	solvent	M_n (g/mol) ^b	D^b	yield (%) ^c
P1	1a	1	MeOH	7600	1.70	93
P2	1a	0.5	MeOH	6000	1.98	68
P3	1a	2	MeOH	8900	1.55	95
P4	1a	1	MeOH/DMSO 2:1	8000	1.59	90
P5	1a	1	MeOH/DMSO 1:1	7700	1.51	91
P6	1a	1	MeOH/DMSO 1:2	6000	1.55	83
P7	1b	1	MeOH	2100	1.45	91
P8	1b	2	MeOH	3700	1.35	82
P9	1c	1	MeOH	6600	1.31	80
P10	1c	2	MeOH	5600	1.31	75

^a[furfural]/[diamine]/[FDCA]/[^tBuNC] = 3/1/1/3. ^bDetermined by SEC with polystyrene as the standard and THF as the eluent. ^cCalculated based on polymers recovered after precipitation.

Scheme 1. Schematic of Ugi-4CP



4 component polymerization.²² Thus, multicomponent polymerization reaction provides a powerful methodology for the direct utilization of biobased chemicals to prepare diverse structural polymers for electronic and biomedical applications.

All the time, PAs are considered to be high-performance polymers due to their outstanding mechanical strength and thermostability. Recent reports have shown that the amide compound without any aromatic structures also has nontraditional intrinsic luminescence (NTIL).^{23–25} Tang et al. reported the nonconventional fluorescent properties of the biogenic and synthetic peptides without aromatic structures and proposed that this fluorescent originated from the hydrogen bonding interactions between the amide groups.²⁶ Maser et al. studied the fluorescence of entangled PA chains and confirmed that the hydrogen bond-mediated supramolecular interactions were the reason for the blue fluorescence phenomena of polymer carbon dots.²⁷ Yang et al. prepared a series of aliphatic PAs with polymerization-induced emissions characteristics by using thiolactone chemistry, in which the intermolecular hydrogen bonding interactions were proposed to explain the origin of their fluorescence.²⁸ In contrast with traditional aromatic fluorescent materials, nonconventional luminophores have enhanced biocompatibility, biodegradability, and water-solubility, which significantly extend their application to bioimaging and drug delivery fields.²⁹ However, the influence of the compositions and structures of aliphatic PAs on their fluorescence behaviors and mechanism has not still been fully understood. Therefore, exploiting rational molecular structures to regulate the fluorescence properties of PA, and further gaining insight into the luminescence mechanism would be desirable and urgently needed.

Here, we utilize furfural-based monomers to construct PAs with NTIL via the Ugi four-component polymerization (Ugi-4CP) and modulate the species and distribution of amides by changing the acid, amine, and aldehyde blocks. Furthermore, the fluorescence properties of PAs can be precisely controlled by the modular design characteristics of the Ugi-4CP. This

protocol not only offers a mild and efficient strategy to construct PAs with various amide units from biobased furfural monomers but also will help us further reveal the structure–emission relationships and NTILs mechanisms.

RESULTS AND DISCUSSION

The Ugi-4CP reaction conditions were optimized by varying the diamine, solvent, and concentration of the monomers, as

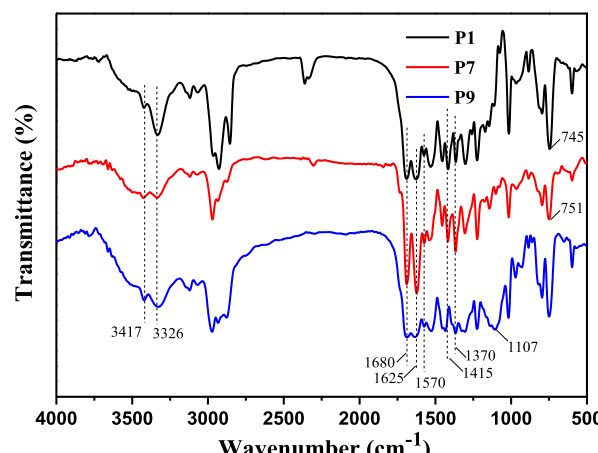


Figure 1. FT-IR spectra of Ugi-4CP products P1, P7, and P9.

shown in Table 1. The reaction mechanism of the Ugi-4CP is proposed in Scheme 1. The polymerization conditions were studied using 1a as a model monomer. As can be seen from Table 1, with the increase of 1a concentration, the yield and molecular weight of the Ugi-4CP products were greatly improved. As a result of the different solubility of the monomers and polymers, the Ugi-4CP reactions in MeOH, dimethyl sulfoxide (DMSO), and their mixture were investigated according to the previous report.¹⁵ The highest yield (93%) and the highest molecular weight ($M_n = 8000$ g mol⁻¹) of the Ugi-4CP products with 1 mol L⁻¹ of 1a

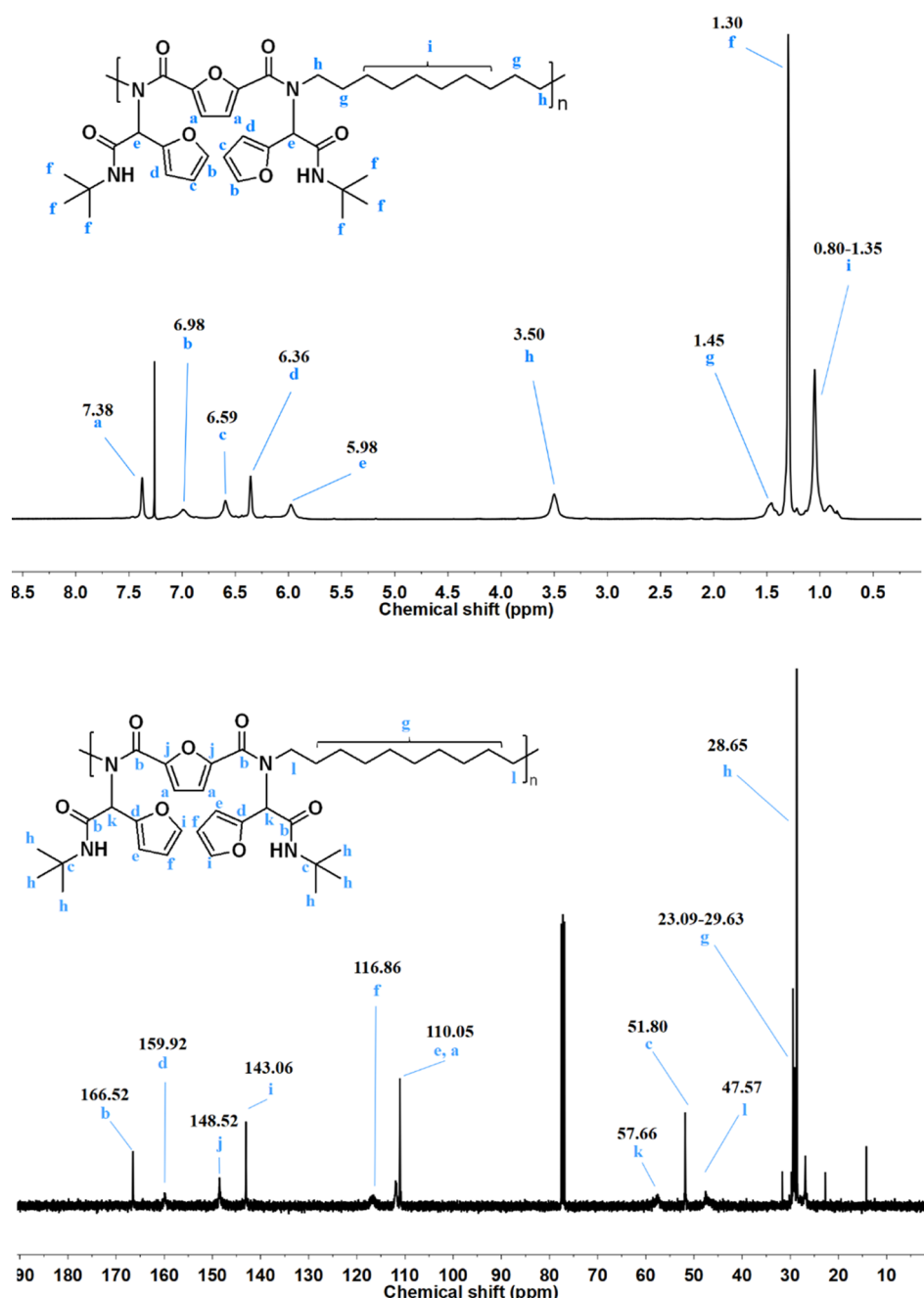


Figure 2. ¹H (up) and ¹³C (down) NMR of P1 in CDCl₃.

monomer were achieved in pure MeOH and a ratio of MeOH/DMSO of 2:1. The detailed characterizations of Ugi-4CP products are described in the following content and Supporting Information.

The structures of P1, P7, and P9 were confirmed by Fourier transform infrared (FT-IR) spectroscopy (Figure 1). The peaks at 1680 and 1625 cm⁻¹ correspond to the typical C=O stretching (band I of amide). The appearance of characteristic peak at 1570 cm⁻¹ is attributed to the band II of amide.^{27,30,31} The bands at 3417 and 3326 cm⁻¹ are assigned to the free and hydrogen-bonded N–H stretching, respectively.^{32,33} In addition, the C=C stretching vibrations in furan structure probably overlaps with the amide characteristic peak.³⁴ The signals at 1415 and 1370 cm⁻¹ correspond to characteristic peaks from the *tert*-butyl groups. The difference in absorption

peaks of the three samples appeared in the fingerprint region of 1400–800 cm⁻¹. The broad band of P9 at 1107 cm⁻¹ corresponds to C–O–C of polyether amine. Compared to P1, the CH₂ stretching peak of P7 blueshifted from 745 to 751 cm⁻¹, which is the result of the shortening of the –CH₂– chain. These results indicate the successful preparation of the Ugi-4CP products.

¹H and ¹³C NMR further confirmed the structure of the Ugi product P1, as shown in Figure 2. The proton peaks from 7.38 to 6.36 ppm in the ¹H NMR spectrum are assigned to the proton of the furan in the backbone and side groups. The signals at 3.50, 1.45, and 1.35–0.80 are related to the long aliphatic chain protons. The *tert*-butyl side group proton is visible at 1.30 ppm. From the ¹³C NMR, the carbonyl carbon chemical shifts of amide on the backbone and side groups are

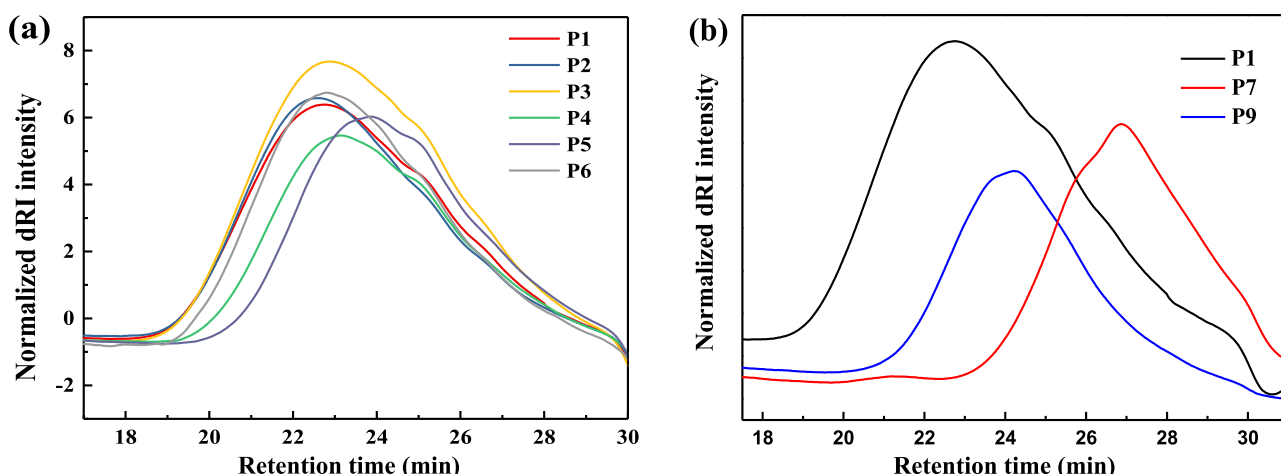


Figure 3. (a) SEC traces of the Ugi-4CP products P1–P6 and (b) SEC traces of the Ugi-4CP products P1, P7, and P9.

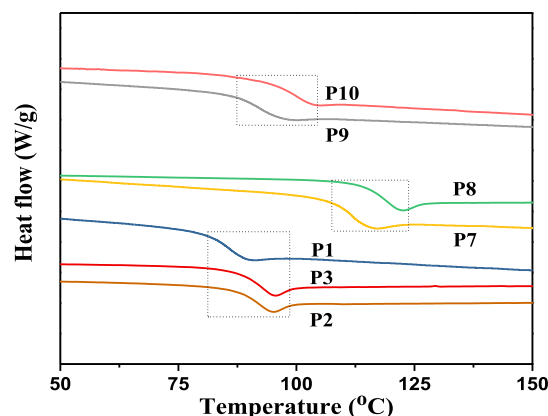


Figure 4. DSC curves of Ugi-4CP products P1–P3 and P7–P10.

observed at 166.52 ppm. More nuclear magnetic resonance (NMR) signals assigned to P1 can be found in Figure 2. The NMR spectra for other Ugi products (P7 and P9) are also shown in Figures S1 and S2.

Subsequently, the effect of polymerization conditions on the structure and molecular weight of the Ugi product was studied, and the results are shown in Table 1 and Figure 3. The molecular weight distributions of the Ugi-4CP products were analyzed via size exclusion chromatography (SEC) with

tetrahydrofuran (THF) as an eluent. Optimization of the reaction parameters was studied with furfural, FDCA, 1,10-diaminododecane, and *tert*-butyl isocyanide as substrates. The influence of the reaction concentration and solvent was investigated. In Figure 3a, SEC (relative calibration) of the Ugi-4CP product samples exhibit a molecular weight in the range of 6000–8900 g mol⁻¹ with a dispersity (*D*) range of 1.51–1.98, depending on the monomer concentration and reaction solvent. Table 1 reveals an increase in the molecular weight and yield of P1 with the increase in concentration, resulting from fewer cyclization reactions.^{14,15,35} The structures and a few macrocycle products for P1, P7, and P9 were confirmed by matrix-assisted laser desorption ionization–time-of-flight–mass spectrometry (MALDI–TOF–MS) (Figure S3). The higher molecular weight ($M_n = 8900$ g mol⁻¹; *D* = 1.55, Table 1, entry P3) was obtained in pure methanol at the concentration of 2 mol L⁻¹. In order to improve the molecular weight, we prepared P8 and P10 with a monomer concentration of 2 mol L⁻¹ (Table 1). Unusually, the high concentration led to the low molecular weight of P10. This is because the high monomer concentration increased the viscosity of the reaction mixture, thereby reducing the mobility of the polymer chains.^{12,15} In Figure 3b, P1 possesses the highest molecular weight with 7600 g mol⁻¹. In contrast, P7 and P9 exhibit molecular weights of 2100 and 6600 g mol⁻¹,

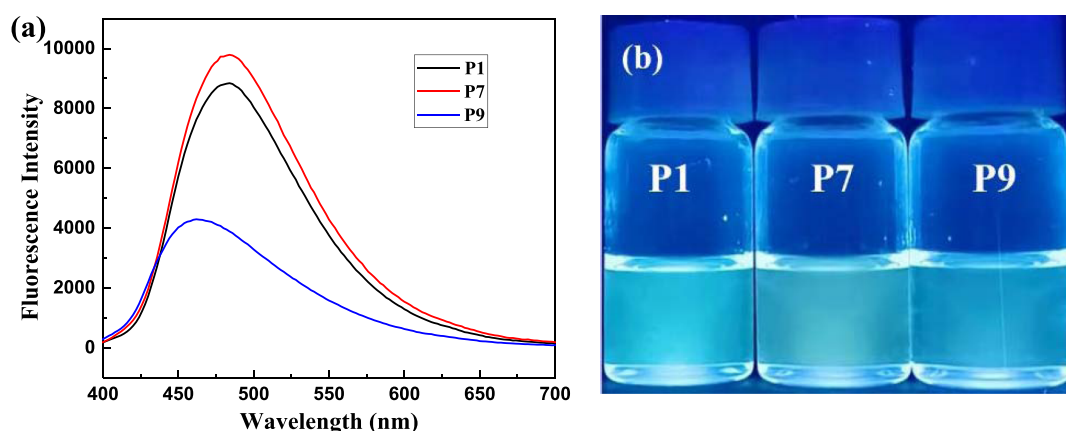


Figure 5. (a) Fluorescence spectra of P1, P7, and P9 (10^{-3} M) in DMF ($\lambda_{ex} = 387$ nm); (b) fluorescence images of P1, P7, and P9 (10^{-3} M) in DMF under a 365 nm UV lamp.

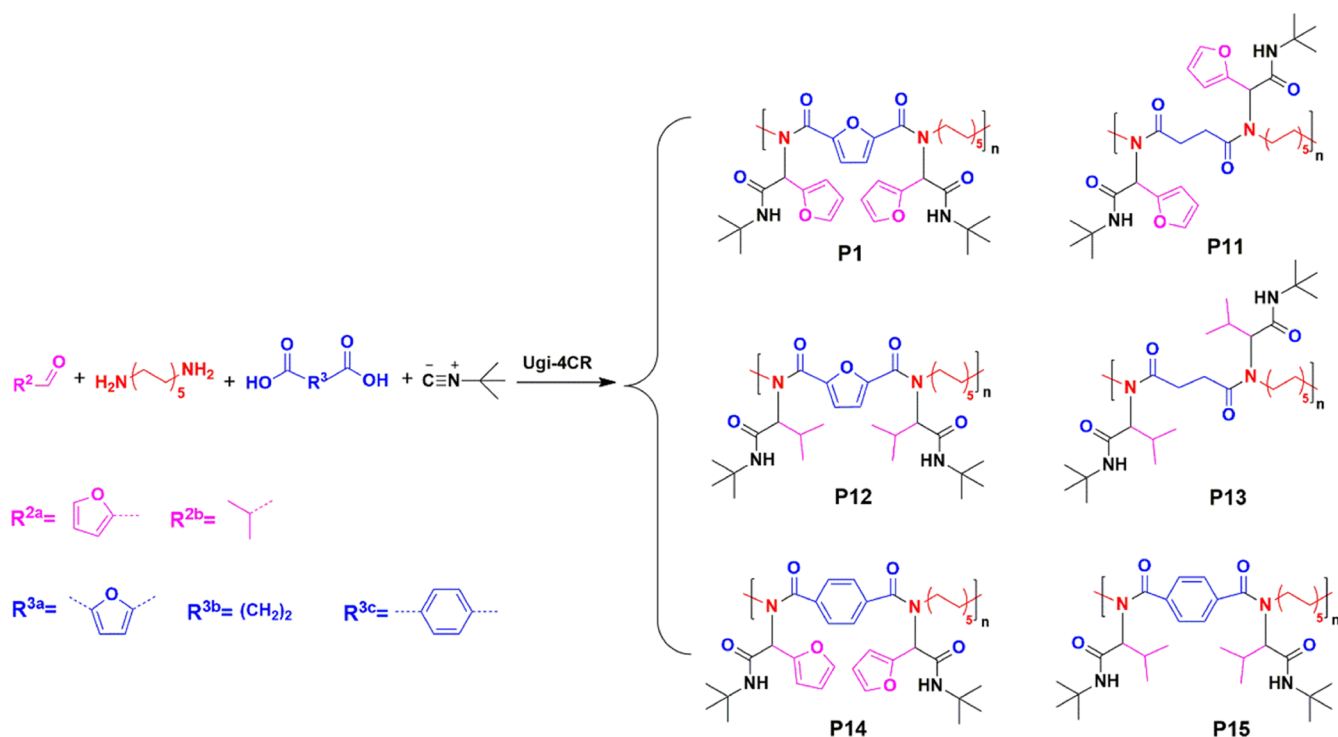
Scheme 2. Ugi-4CP With 1,10-Diaminodecane, Aldehyde 2a–2b, Dicarboxylic Acid 3a–3c, and *tert*-butyl Isocyanide

Table 2. Characterization of the Ugi-4CP (P11–P16)

polymer	P11	P12	P13	P14	P15	P16
$\lambda_{\text{ex}} \text{ (nm)}$	380	N ^a	N	383	N	N
$\lambda_{\text{em}} \text{ (nm)}$	464	N	N	477	N	N
$M_n \text{ (g/mol)}$	3400	5300	17,500	5300	11,200	4600
D^b	1.75	1.77	1.55	1.48	1.63	1.75

^aN: no signal. ^bDetermined by SEC with polystyrene as the standard and THF as the eluent.

respectively. The molecular weights of the furfural-based PAs prepared by Ugi-4CP are equivalent to that of previously reported Ugi products in the literature.^{12–22}

The thermal characterization of the Ugi-4CP products is conducted via DSC (Figure 4). The DSC measurements show that the P1–P3, P7–P8, and P9–P10 products possess a glass transition temperature (T_g) of 85.9–92.0, 111.9–118.4, and 92.3–99.4 °C, respectively. The small effect of changing the molecular weight on the T_g value of Ugi-4CP products can be observed. The presence of the long alkyl group (P1–P3)

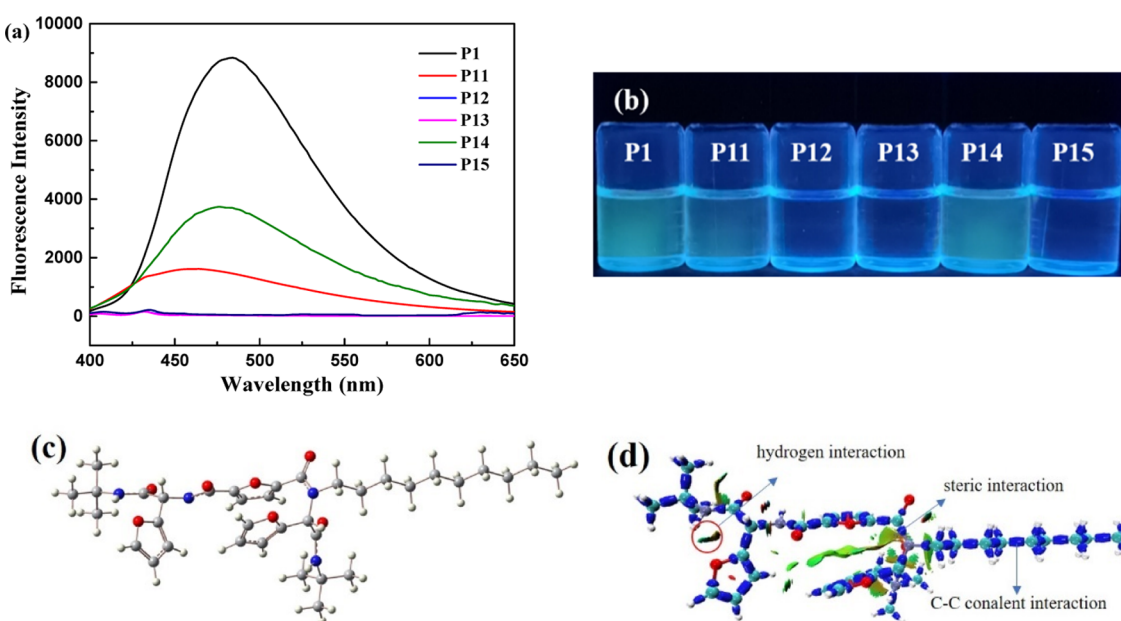


Figure 6. (a) Fluorescence spectra of P1 and P11–P15 (10^{-3} M) in DMF, (b) fluorescence images of P1 and P11–P15 (10^{-3} M) in DMF under a 365 nm UV lamp, (c) optimized structure of the P1 repeating unit, and (d) interaction region indicator maps of the P1 repeating unit.

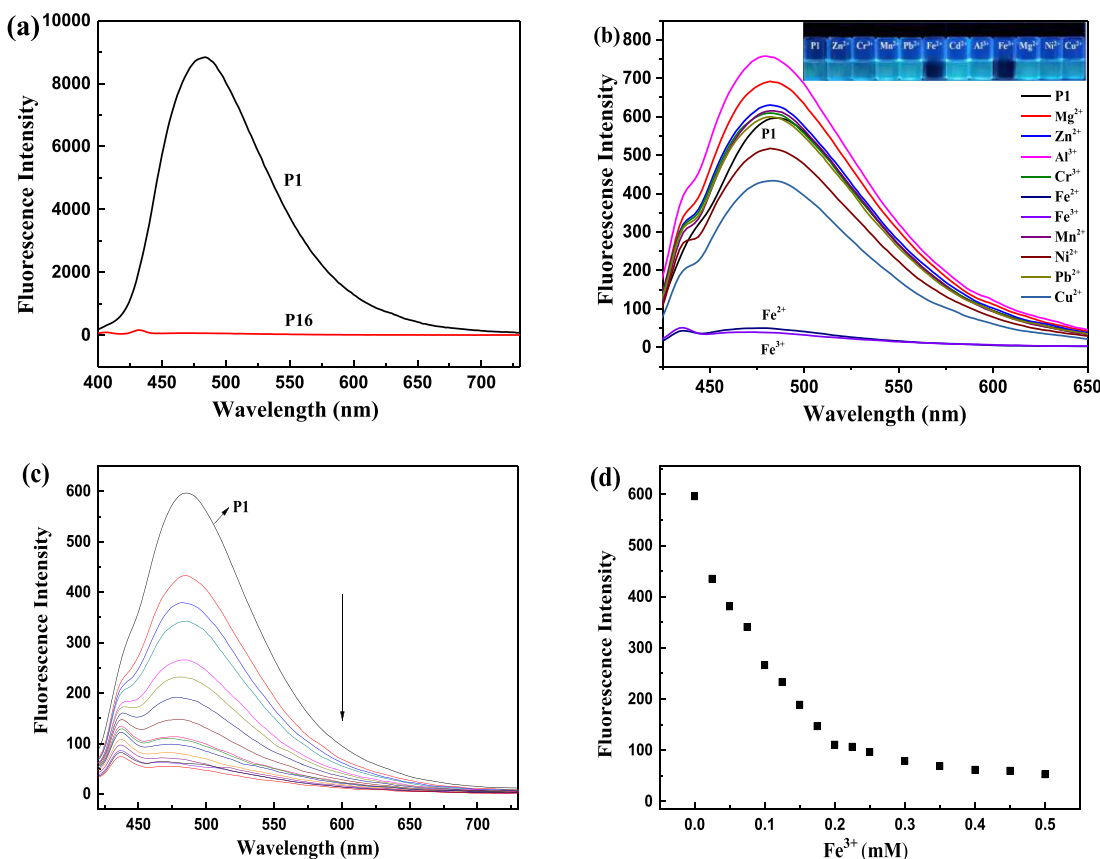
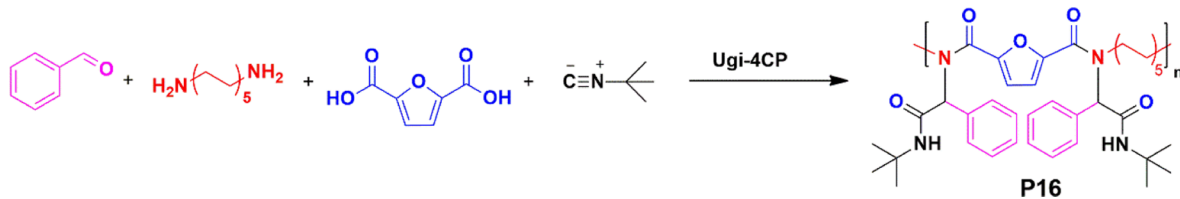
Scheme 3. Ugi-4CP with Benzaldehyde, 1,10-Decanediamine, FDCA, and *tert*-butyl Isocyanide

Figure 7. (a) Fluorescence spectra of P1 and P16 (10^{-3} M) in DMF; (b) emission spectra of P1 in DMF with different metal ions (inset: photo of P1 (10^{-3} M) in DMF with 5.0 equiv of different metal ions under a 365 nm UV lamp); (c) fluorescence spectra of P1 with various concentrations of Fe^{3+} in the DMF– H_2O mixture (7:3, v/v); (d) fluorescence intensity at 484 nm alterations with the concentrations of Fe^{3+} in the DMF– H_2O mixture (7:3, v/v) ($\lambda_{\text{ex}} = 387$ nm).

lowered the T_g . P7–P8 with the short alkyl group showed the highest T_g values because of the highest rigidity, which inhibits the molecular motion.

The photoluminescence spectra of the Ugi-4CP products in N,N -dimethyl formamide (DMF) (10^{-3} mol L^{-1}) are shown in Figure 5a. The polymers exhibit strong absorption at 460–484 nm, which is attributed to the electron delocalization caused by hydrogen bonding interactions.^{36,37} The intramolecular/intermolecular interactions can rigidify molecular conformations and diminish nonradiative deactivation, thus featuring photoluminescence characteristics.^{38–40} As illustrated in Figure 5a, λ_{em} of P1, P7, and P9 polymers in DMF solutions are 484, 484, and 460 nm. The blue shift of the P9 compared with the P1 and P7 could be attributed to the additional oxygen atoms from polyether amine in the P9 main chain.²⁸ The fluorescence photograph of the Ugi-4CP products under the illumination of a 365 nm UV lamp is shown in Figure 5b. The effect of molecular weight (M_n) of P1, P7, and P9 on their fluorescence intensity was investigated, as shown in Figure S4. The P1 with

moderate M_n exhibited the strongest fluorescence intensity, and the fluorescence intensity of P7 and P9 increased with the increase of M_n .

Note that the dilute solutions of nonconventional luminophores are nonemissive, but their fluorescence can be a boost in concentrated solutions and/or the solid state, showing aggregation-induced emission characteristics.²⁹ Analyzing the structure of P1, P7, and P9, we speculate that furan structure and amide groups jointly participate in the construction of chromophores through intramolecular hydrogen bonds. To investigate the fluorescence emission mechanism of PAs, the furan structure of P1 in backbone and side groups was replaced with aliphatic and benzene ring substituents by the modular characteristics of the Ugi reaction, as shown in Scheme 2. The obtained PAs (P11–P15) were characterized in detail using FT-IR, NMR, and SEC (for detailed information, see Supporting Information and Table 2).

The effects of furfural derivatives monomers on PAs fluorescence are shown in Figure 6. P1, P11, and P14 exhibit obvious fluorescence emission behaviors. In contrast, P12, P13, and P15 have no obvious fluorescence emission signal in DMF. To further clarify the relationship between the structure and fluorescence emission of these polymers, density functional theory calculations have been performed on the repeating unit of the P1. The optimized structures confirmed the establishment of intramolecular hydrogen bonds (Figure 6c,d). Therefore, the strong fluorescence of P1, P11, and P14 comes from the formation of an intramolecular hydrogen bond (stable six-membered rings) between secondary amide and furan oxygen atom in the side groups, as shown in Figure 6d. In addition, 2,5-furan dicarboxylic acid and terephthalic acid have a similar steric effect, but P1 has stronger fluorescence intensity than P14. It is speculated that the furan group in the backbone may also participates in the formation of hydrogen bonds. Furthermore, P12 contained a furan group only in the backbone and did not show an obvious fluorescence signal. Therefore, the intramolecular hydrogen bonds formed by the pendant furfural groups are essential for the photoluminescence properties of the Ugi-4CP products.

The fluorescence mechanism of PAs is further verified by the comparative experiments (Scheme 3). We synthesized P16 from benzaldehyde instead of furfural, and its fluorescence disappeared due to the lack of intramolecular hydrogen bond interaction as expected (Figure 7a and Table 2). To explore the potential application of fluorescent PAs, we used P1 with strong fluorescence characteristics and high yield as the probe to detect metal ions. Free probe P1 shows a strong fluorescence emission at 484 nm (Figure 7b, $\lambda_{ex} = 387$ nm). Subsequently, various metal ions (5.0 equiv) such as Zn^{2+} , Cr^{3+} , Mn^{2+} , Pb^{2+} , Fe^{2+} , Al^{3+} , Fe^{3+} , Mg^{2+} , Ni^{2+} , and Cu^{2+} , were added to P1 (10^{-4} M). Notably, the metal ions show a slight effect on the emission intensity of the P1 probe, but only Fe^{2+} and Fe^{3+} exhibit a significant fluorescence quenching effect, which can be directly observed by the naked eye, as shown in the inset of Figure 7b. It is well known that fluorescence quenching is related to the specific interaction between the probe and the metal ions. Due to unconventional fluorescence of PAs results from hydrogen bonding interactions, the P1 probe exhibits a distinct fluorescence response, which can be ascribed to the complexation of Fe^{2+} (or Fe^{3+}) with oxygen or nitrogen atom.^{41,42} Fe^{3+} plays an important role in human metabolism and oxygen uptake, so it is of great significance to develop an Fe^{3+} detector and biosensor.⁴³ Figure 7c,d show the typical optical response of the P1 probe (10^{-4} M) to incremental Fe^{3+} (0–0.5 mM). As a result of the complexation interaction between the P1 probe and Fe^{3+} , the fluorescence intensity of the probe at 484 nm is significantly decreased with the titration of Fe^{3+} . The present P1 probe exhibits superior or comparable sensitivity to other nontraditional fluorescent polymer probes in the previous report.^{44–46} This result demonstrates that the P1 probe could be used for rapid and sensitive monitoring of Fe^{3+} in an aqueous solution.

CONCLUSIONS

In summary, we synthesized furfural-based PA with the desired fluorescence properties by Ugi multicomponent polymerization. The fluorescence mechanism was investigated by changing the multicomponent reaction module and the optimized structures. The experimental and theoretical results prove that the strong fluorescence of PA comes from the

intramolecular hydrogen bond between the secondary amide and furan oxygen atom in the side groups. By summarizing the polymerization results, Ugi-4CP has been shown as a novel tool from renewable furfural derivatives monomer to synthesize PA with NTIL. The PA probe displays high selectivity for Fe^{2+} and Fe^{3+} among various metal ions by significantly reduced fluorescence. Therefore, the furfural-based PAs synthesized in this study can be used as fluorescence probes of Fe^{2+} and Fe^{3+} with high sensitivity and selectivity for the biomedical field in the future.

ASSOCIATED CONTENT

Supporting Information

The Supporting Information is available free of charge at <https://pubs.acs.org/doi/10.1021/acs.macromol.2c01214>.

Additional experimental details, FT-IR, NMR, and MALDI–TOF–MS spectra (PDF)

AUTHOR INFORMATION

Corresponding Authors

Xue Wang – College of Chemistry and Chemical Engineering, Yantai University, Yantai 264005, PR China;  orcid.org/0000-0003-3444-733X; Email: wangxue@ytu.edu.cn

Yusheng Qin – College of Chemistry and Chemical Engineering, Yantai University, Yantai 264005, PR China;  orcid.org/0000-0002-9183-5657; Email: ysqin@ytu.edu.cn

Authors

Chang Liu – College of Chemistry and Chemical Engineering, Yantai University, Yantai 264005, PR China

Zhihao Xing – College of Chemistry and Chemical Engineering, Yantai University, Yantai 264005, PR China

Hongyi Suo – College of Chemistry and Chemical Engineering, Yantai University, Yantai 264005, PR China

Rui Qu – College of Chemistry and Chemical Engineering, Yantai University, Yantai 264005, PR China

Qingzhong Li – College of Chemistry and Chemical Engineering, Yantai University, Yantai 264005, PR China;  orcid.org/0000-0003-1486-6772

Complete contact information is available at: <https://pubs.acs.org/10.1021/acs.macromol.2c01214>

Notes

The authors declare no competing financial interest.

ACKNOWLEDGMENTS

This research was supported by the Natural Science Foundation of Shandong Province (ZR2020QE088), National Natural Science Foundation of China (52073244), Taishan Scholar Program (TSQN201909086), and Central Government Special Funds Supporting the Development of Local Science and Technology (YDZX2020370001726).

REFERENCES

- (1) Bozell, J. J.; Petersen, G. R. Technology development for the production of biobased products from biorefinery carbohydrates—the US Department of Energy's "Top 10" revisited. *Green Chem.* **2010**, *12*, 539–554.
- (2) Ragauskas, A. J.; Williams, C. K.; Davison, B. H.; Britovsek, G.; Cairney, J.; Eckert, C. A.; Frederick, W. J., Jr.; Hallett, J. P.; Leak, D. J.; Liotta, C. L.; Mielenz, J. R.; Murphy, R.; Templar, R.; Tschaplinski, J.

T. The path forward for biofuels and biomaterials. *Science* **2006**, *311*, 484–489.

(3) de Jong, E.; Dam, M. A.; Sipos, L.; Gruter, G. J. M. Furandicarboxylic acid (FDCA), a versatile building block for a very interesting class of polyesters. In: Biobased monomers, polymers, and materials. *ACS Symp. Ser.* **2012**, *1105*, 1–13.

(4) Gomes, M.; Gandini, A.; Silvestre, A. J. D.; Reis, B. Synthesis and characterization of poly(2,5-furan dicarboxylate)s based on a variety of diols. *J. Polym. Sci., Part A: Polym. Chem.* **2011**, *49*, 3759–3768.

(5) *Top Value Added Chemicals from Biomass: Volume 1-results of Screening for Potential Candidates from Sugars and Synthetic Gas*; Werpy, T., Petersen, G., Eds.; U.S. Department of Energy: Washington, 2004.

(6) Kakuchi, R. Multicomponent reactions in polymer synthesis. *Angew. Chem., Int. Ed.* **2014**, *53*, 46–48.

(7) Espeel, P.; Goethals, F.; Du Prez, F. E. One-pot multistep reactions based on thiolactones: extending the realm of thiol-ene chemistry in polymer synthesis. *J. Am. Chem. Soc.* **2011**, *133*, 1678–1681.

(8) Kreye, O.; Tóth, T.; Meier, M. A. R. Introducing multicomponent reactions to polymer science: Passerini reactions of renewable monomers. *J. Am. Chem. Soc.* **2011**, *133*, 1790–1792.

(9) Xue, H. D.; Zhao, Y.; Wu, H. B.; Wang, Z. L.; Yang, B.; Wei, Y.; Wang, Z. M.; Tao, L. Multicomponent combinatorial polymerization via the Biginelli reaction. *J. Am. Chem. Soc.* **2016**, *138*, 8690–8693.

(10) Kreye, O.; Türünç, O.; Sehlinger, A.; Rackwitz, J.; Meier, M. A. R. Structurally diverse polyamides obtained from monomers derived via the Ugi multicomponent reaction. *Chem.—Eur. J.* **2012**, *18*, 5767–5776.

(11) Ugi, I.; Steinbrückner, C. Über ein neues Kondensations-Prinzip. *Angew. Chem.* **1960**, *72*, 267–268.

(12) Sehlinger, A.; Dannecker, P. K.; Kreye, O.; Meier, M. A. R. Diversely substituted polyamides: macromolecular design using the Ugi four-component reaction. *Macromolecules* **2014**, *47*, 2774–2783.

(13) Yang, B.; Zhao, Y.; Fu, C. K.; Zhu, C. Y.; Zhang, Y. L.; Wang, S. Q.; Wei, Y.; Tao, L. Introducing the Ugi reaction into polymer chemistry as a green click reaction to prepare middle-functional block copolymers. *Polym. Chem.* **2014**, *5*, 2704–2708.

(14) Hartweg, M.; Becer, R. C. Direct polymerization of levulinic acid via Ugi multicomponent reaction. *Green Chem.* **2016**, *18*, 3272–3277.

(15) Schade, O. R.; Dannecker, P.; Kalz, K. F.; Steinbach, D.; Meier, M. A. R.; Grunwaldt, J. Direct catalytic route to biomass-derived 2,5-furandicarboxylic acid and its use as monomer in a multicomponent polymerization. *ACS Omega* **2019**, *4*, 16972–16979.

(16) Zhang, X. J.; Wang, S. H.; Liu, J.; Xie, Z. G.; Luan, S. F.; Xiao, C. S.; Tao, Y. H.; Wang, X. H. Ugi reaction of natural amino acids: a general route toward facile synthesis of polypeptoids for bioapplications. *ACS Macro Lett.* **2016**, *5*, 1049–1054.

(17) Tao, Y.; Wang, S. X.; Zhang, X. J.; Wang, Z.; Tao, Y. H.; Wang, X. H. Synthesis and properties of alternating polypeptoids and polyampholytes as protein-resistant polymers. *Biomacromolecules* **2018**, *19*, 936–942.

(18) Tao, Y.; Chen, J. L.; Wang, S. X.; Tao, Y. H. Direct polymerization of lysine and furfural via Ugi reaction. *Acta Polym. Sin.* **2020**, *51*, 738–743.

(19) Zhu, Y. N.; Tao, Y. H. Sequence-controlled and sequence-defined polypeptoids via the Ugi reaction: synthesis and sequence-driven properties. *Polym. Chem.* **2021**, *12*, 4895–4902.

(20) Al Samad, A.; De Winter, J.; Gerbaux, P.; Jérôme, C.; Debuigne, A. Unique alternating peptide-peptoid copolymers from dipeptides via Ugi reaction in water. *Chem. Commun.* **2017**, *53*, 12240–12243.

(21) Stiernet, P.; Couturaud, B.; Bertrand, V.; Eppe, G.; De Winter, J.; Debuigne, A. Ugi four-component polymerization of amino acid derivatives: a combinatorial tool for the design of polypeptoids. *Polym. Chem.* **2021**, *12*, 2141–2151.

(22) MacKinnon, D.; Zhao, T.; Becer, C. R. Tuneable N-substituted polyamides with high biomass content via Ugi 4 component polymerization. *Macromol. Chem. Phys.* **2022**, *223*, 2100408.

(23) Tomalia, D. A.; Klajnert-Maculewicz, B.; Johnson, K. A. M.; Brinkman, H. F.; Janaszewska, A.; Hedstrand, D. M. Non-traditional intrinsic luminescence: inexplicable blue fluorescence observed for dendrimers, macromolecules and small molecular structures lacking traditional/conventional luminophores. *Prog. Polym. Sci.* **2019**, *90*, 35–117.

(24) Liu, B.; Zhang, H. K.; Liu, S. J.; Sun, J. Z.; Zhang, X. H.; Tang, B. Z. Polymerization-induced emission. *Mater. Horiz.* **2020**, *7*, 987–998.

(25) Larson, C. L.; Tucker, S. A. Intrinsic fluorescence of carboxylate-terminated polyamido amine dendrimers. *Appl. Spectrosc.* **2001**, *55*, 679–683.

(26) Ye, R. Q.; Liu, Y. Y.; Zhang, H. K.; Su, H. F.; Zhang, Y. L.; Xu, L. G.; Hu, R. R.; Kwok, R. T. K.; Wong, K. S.; Lam, J. W. Y.; Goddard, W. A.; Tang, B. Z. Non-conventional fluorescent biogenic and synthetic polymers without aromatic rings. *Polym. Chem.* **2017**, *8*, 1722–1727.

(27) Vallan, L.; Urriolabeitia, E. P.; Ruipérez, F.; Matxain, J. M.; Canton-Vitoria, R.; Tagmatarchis, N.; Benito, A. M.; Maser, W. K. Supramolecular-enhanced charge transfer within entangled polyamide chains as the origin of the universal blue fluorescence of polymer carbon dots. *J. Am. Chem. Soc.* **2018**, *140*, 12862–12869.

(28) Yan, J. J.; Wang, X. Y.; Xiong, J. J.; Wang, L. Z.; Pan, D. H.; Xu, Y. P.; Yang, M. Uncovering divergent fluorescence of aliphatic polyamides: Synthesis, dual polymerization-induced emissions, and organelle-specific imaging. *Chem. Eng. J.* **2022**, *428*, 132142.

(29) Tang, S.; Yang, T.; Zhao, Z.; Zhu, T.; Zhang, Q.; Hou, W.; Yuan, W. Z. Nonconventional luminophores: characteristics, advancements and perspectives. *Chem. Soc. Rev.* **2021**, *50*, 12616–12655.

(30) Porubská, M.; Szöllősi, O.; Kónová, A.; Janigová, I.; Jašková, M.; Jomová, K.; Chodák, I. FTIR spectroscopy study of polyamide-6 irradiated by electron and proton beams. *Polym. Degrad. Stabil.* **2012**, *97*, 523–531.

(31) Kang, H. L.; Wang, Z.; Hao, X. M.; Liu, R. G. Thermal induced crystalline transition of bio-based polyamide 56. *Polymer* **2022**, *242*, 124540.

(32) Skrovanek, D. J.; Howe, S. E.; Painter, P. C.; Coleman, M. M. Hydrogen bonding in polymers: infrared temperature studies of an amorphous polyamide. *Macromolecules* **1985**, *18*, 1676–1683.

(33) Coleman, M. M.; Lee, K. H.; Skrovanek, D. J.; Painter, P. C. Hydrogen bonding in polymers. 4. Infrared temperature studies of a simple polyurethane. *Macromolecules* **1986**, *19*, 2149–2157.

(34) Fu, W. Q.; Kong, L. W.; Shi, J. B.; Tong, B.; Cai, Z. X.; Zhi, J. G.; Dong, Y. P. Synthesis of poly(amine-furan-arylene)s through a one-pot catalyst-free in situ cyclopolymerization of diisocyanide, dialkylacetylene dicarboxylates, and dialdehyde. *Macromolecules* **2019**, *52*, 729–737.

(35) Dannecker, P. K.; Sehlinger, A.; Meier, M. A. R. Polymacrocycles derived via Ugi multi-component reactions. *Macromol. Rapid Commun.* **2019**, *40*, 1800748.

(36) Shukla, A.; Mukherjee, S.; Sharma, S.; Agrawal, V.; Radha Kishan, K. V. R.; Guptasarma, P. A novel UV laser-induced visible blue radiation from protein crystals and aggregates: scattering artifacts or fluorescence transitions of peptide electrons delocalized through hydrogen bonding? *Arch. Biochem. Biophys.* **2004**, *428*, 144–153.

(37) Jiang, N.; Zhu, D. X.; Su, Z. M.; Bryce, M. R. Recent advances in oligomers/polymers with unconventional chromophores. *Mater. Chem. Front.* **2021**, *5*, 60–75.

(38) Yuan, W. Z.; Zhang, Y. Nonconventional macromolecular luminogens with aggregation-induced emission characteristics. *J. Polym. Sci., Part A: Polym. Chem.* **2017**, *55*, 560–574.

(39) Chen, X.; Wang, Y.; Zhang, Y.; Yuan, W. Z. Clustering-triggered emission of nonconventional luminophores. *Prog. Chem.* **2019**, *31*, 1560–1575.

(40) Wang, Y.; Zhao, Z.; Yuan, W. Z. Intrinsic luminescence from nonaromatic biomolecules. *ChemPlusChem* **2020**, *85*, 1065–1080.

(41) Sigel, H.; Martin, R. B. Coordinating properties of the amide bond. Stability and structure of metal ion complexes of peptides and related ligands. *Chem. Rev.* **1982**, *82*, 385–426.

(42) Bai, L. H.; Yan, H. X.; Feng, Y. B.; Feng, W. X.; Yuan, L. Y. Multi-excitation and single color emission carbon dots doped with silicon and nitrogen: synthesis, emission mechanism, Fe^{3+} probe and cell imaging. *Chem. Eng. J.* **2019**, *373*, 963–972.

(43) Chu, B.; Zhang, H. K.; Hu, L. F.; Liu, B.; Zhang, C. J.; Zhang, X. H.; Tang, B. Z. Altering Chain Flexibility of Aliphatic Polyesters for Yellow-Green Clusteroluminescence in 38% Quantum Yield. *Angew. Chem., Int. Ed.* **2022**, *61*, No. e202114117.

(44) Yuan, L. Y.; Yan, H. Y.; Bai, L. H.; Bai, T.; Zhao, Y.; Wang, L.; Feng, Y. B. Unprecedented multicolor photoluminescence from hyperbranched poly(amino ester)s. *Macromol. Rapid Commun.* **2019**, *40*, 1800658.

(45) Du, Y. Q.; Yan, H. X.; Huang, W.; Chai, F.; Niu, S. Unanticipated strong blue photoluminescence from fully bio-based aliphatic hyperbranched polyesters. *ACS Sustainable Chem. Eng.* **2017**, *5*, 6139–6147.

(46) Wang, Y. Z.; Bin, X.; Chen, X. H.; Zheng, S. Y.; Zhang, Y. M.; Yuan, W. Z. Emission and emissive mechanism of nonaromatic oxygen clusters. *Macromol. Rapid Commun.* **2018**, *39*, 1800528.

□ Recommended by ACS

Structure-Dependent Nontraditional Intrinsic Fluorescence of Aliphatic Hyperbranched Polyureas

Yao Luo, Jun Yue, *et al.*

JUNE 21, 2022

BIOCONJUGATE CHEMISTRY

READ 

Hydrogen-Bonding-Induced Clusteroluminescence and UCST-Type Thermoresponsiveness of Nonconjugated Copolymers

Kang Liu, Chuanzhuang Zhao, *et al.*

SEPTEMBER 30, 2022

MACROMOLECULES

READ 

A Universal Strategy for Producing Fluorescent Polymers Based on Designer Hyperbranched Polyethylene Ternary Copolymers

Jinwei Song, Lixin Xu, *et al.*

MARCH 01, 2022

MACROMOLECULES

READ 

Next-Generation High-Performance Biobased Naphthalate-Modified PET for Sustainable Food Packaging Applications

Ting-Han Lee, Eric W. Cochran, *et al.*

AUGUST 24, 2022

MACROMOLECULES

READ 

Get More Suggestions >